

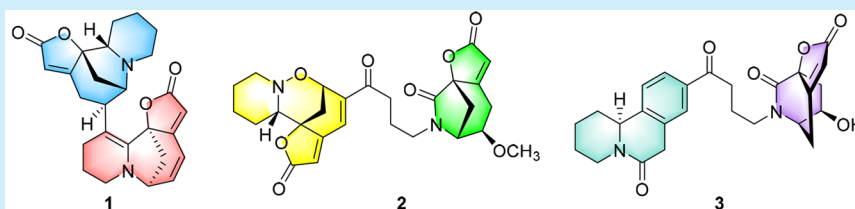
# Flueggeacosines A–C, Dimeric Securinine-Type Alkaloid Analogues with Neuronal Differentiation Activity from *Flueggea suffruticosa*

Zhen-Long Wu,<sup>†,‡,§</sup> Xiao-Jun Huang,<sup>†,‡,§</sup> Ming-Tao Xu,<sup>†,‡</sup> Xuanyue Ma,<sup>‡</sup> Liuren Li,<sup>‡</sup> Lei Shi,<sup>‡</sup> Wen-Jing Wang,<sup>‡</sup> Ren-Wang Jiang,<sup>†,‡</sup> Wen-Cai Ye,<sup>\*,†,‡,§</sup> and Ying Wang<sup>\*,†,‡,§</sup>

<sup>†</sup>Institute of Traditional Chinese Medicine & Natural Products, College of Pharmacy, Jinan University, Guangzhou 510632, People's Republic of China

<sup>‡</sup>Guangdong Province Key Laboratory of Pharmacodynamic Constituents of TCM & New Drugs Research, Jinan University, Guangzhou 510632, People's Republic of China

## Supporting Information



**ABSTRACT:** Flueggeacosines A–C (1–3), three dimeric securinine-type alkaloid analogues with unprecedented skeletons, were isolated from *Flueggea suffruticosa*. Compounds 1 and 2 are the first examples of C-3–C-15' connected dimeric securinine-type alkaloids. Compound 3 is an unprecedented heterodimer of securinine-type and benzoquinolizidine alkaloids. Biosynthetic pathways for 1–3 were proposed on the basis of the coexisting alkaloid monomers as the precursors. Compound 2 exhibited significant activity in promoting neuronal differentiation of Neuro-2a cells.

The *Securinega* alkaloids are an emerging group of plant-derived indolizidine alkaloids with promising bioactivities for central nervous system (CNS), antitumor, and antibacterium.<sup>1–3</sup> Commonly, these alkaloids feature a unique bridged tetracyclic core, including a piperidine (or pyrrole) ring (ring A), a fused azabicyclo[3.2.1] or azabicyclo[2.2.2] octane ring (rings B and C), and a butenolide moiety (ring D). According to the size of ring A, the *Securinega* alkaloids are usually classified into two main subgroups: securinine-type (ring A is a piperidine, Figure 1) and norsecurinine-type (ring A is a pyrrole).<sup>1</sup> In the recent years, more than 30 oligomeric *Securinega* alkaloids spanning from dimers to pentamers had

been characterized.<sup>4,5</sup> Interestingly, almost all of these oligomers were derived from norsecurinine-type alkaloids via C-12, C-14, or C-15 positions. However, oligomers derived from securinine-type alkaloids are rarely reported so far.

Our previous studies on the genus *Flueggea* had led to the isolation of flueggeanine, the sole case of dimeric securinine-type alkaloid, which is presumably biosynthesized via a [2 + 2] cycloaddition reaction between two molecules of virosecurinine.<sup>6</sup> In our continuing research, three novel dimeric securinine-type alkaloid analogues, flueggeacosines A–C (1–3), along with their putative biosynthetic precursors [securinine (4), allosecurinine (5), and 15 $\beta$ -methoxy-14,15-dihydroviroallosecurinine (6)] were isolated from the roots of *Flueggea suffruticosa* (Figure 1). Structurally, compounds 1 and 2 represent the first members of two new classes of dimeric securinine-type alkaloids with an unprecedented C-3–C-15' linkage. Notably, the unusual dimerization pattern in 1 resulted in the presence of a rare configurationally stable alkenyl-Csp<sup>3</sup> chiral axis, while compound 2 possesses a unique ring A opened securinine-type alkaloid motif. Compound 3 is an unprecedented heterodimer of securinine-type (ring A opened) and benzoquinolizidine alkaloids. Herein, we report the isolation, structural elucidation, and the hypothetical pathways of these novel alkaloids. Additionally, their activities

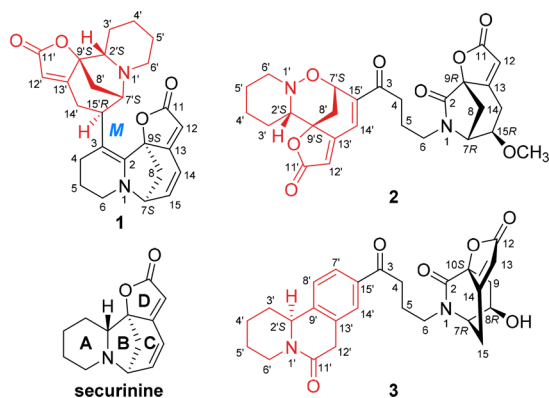


Figure 1. Chemical structures of 1–3 and securinine.

Received: October 26, 2018

Published: November 28, 2018

for regulating the morphology of Neuro-2a cells were also evaluated.

Flueggeacosine A (**1**) was isolated as orange needles. The molecular formula of **1** was established as  $C_{26}H_{28}N_2O_4$  based on its HR-ESI-MS data ( $m/z$  433.2133  $[M + H]^+$ , calcd for  $C_{26}H_{29}N_2O_4$ : 433.2122). The  $^1H$  and  $^{13}C$  NMR data of **1** revealed the presence of signals for two monomeric securinine-type alkaloids, including two typical  $\alpha,\beta$ -unsaturated  $\gamma$ -lactone rings, a disubstituted double bond, and a tetrasubstituted double bond. The above spectral data combined with the molecular formula information suggested that **1** was a dimeric securinine-type alkaloid. Based on comprehensive analysis of  $^1H$ - $^1H$  COSY, HSQC, and HMBC spectra, the  $^1H$  and  $^{13}C$  NMR data of **1** were assigned and shown in Table S1 (see the Supporting Information).

The  $^1H$ - $^1H$  COSY spectrum of **1** displayed the presence of four spin-coupling systems ( $H_2-4$  to  $H_2-6$ ,  $H_2-8$  to  $H_2-14$ ,  $H_2-2'$  to  $H_2-6'$ , and  $H_2-8'$  to  $H_2-14'$ ). In the HMBC spectrum, the correlations between  $H_2-7$  and  $C-2/C-6/C-9$ , between  $H_2-8$  and  $C-2/C-13$ , between  $H_2-12$  and  $C-9/C-14$ , between  $H_2-15$  and  $C-13$ , between  $H_2-2'$  and  $C-6'/C-7'/C-8'/C-13'$ , between  $H_2-7'$  and  $C-6'/C-9'$ , as well as between  $H_2-12'$  and  $C-9'/C-14'$  were observed. The above data suggested that **1** possessed two monomeric securinine-type alkaloid units. Furthermore, the HMBC correlations between  $H_2-15'$  and  $C-2/C-4$  indicated that the two units were connected through  $C-3$  and  $C-15'$ . Thus, the planar structure of **1** was established as shown in Figure 2.

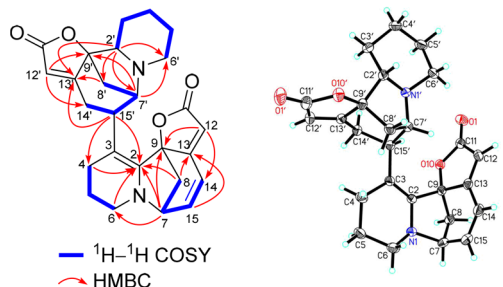


Figure 2. Key 2D NMR correlations and X-ray ORTEP drawing of **1**.

Crystals of **1** for single-crystal X-ray diffraction were acquired from  $MeOH-CHCl_3$  (1:1). In the X-ray structure of **1** [Cu  $K\alpha$ , Flack parameter = 0.04(13)], the two bulky monomeric *Securinega* alkaloid units adopt a fairly fixed and somewhat “anti” relationship, resulting in the formation of a rare alkenyl- $Csp^3$  chiral axis along the  $C-3-C-15'$  bond. Interestingly, the obvious NOE correlations between  $H_2-4$  and  $H_2-8'$ / $H_2-14'$  suggested that this alkenyl- $Csp^3$  chiral axis could stably exist in solution at room temperature and was determined to be *M*-configured.<sup>7</sup> Moreover, the result of conformational distribution analysis of **1** indicated that only the 3*M*-configuration could actually occur at room temperature because of its predominantly thermodynamic stability (with a population of 100% for 3*M*-configuration, Table S2). Employing the noncovalent interaction (NCI) analysis,<sup>8</sup> the significant hydrogen-bond and van der Waals interactions between the two fragments further confirmed the stability of 3*M*-configuration for **1** (Figures S1 and S2). Hence, the absolute configuration of **1** was determined to be 3*M*,7*S*,9*S*,2'*S*,7'*S*,9'*S*,15'*R*.

The molecular formula of flueggeacosine B (**2**) was deduced to be  $C_{27}H_{30}N_2O_8$  on the basis of its HR-ESI-MS at  $m/z$  511.2078  $[M + H]^+$  (calcd for  $C_{27}H_{31}N_2O_8$ : 511.2080). Analysis of the  $^1H$  and  $^{13}C$  NMR spectra of **2** revealed the presence of a ketone carbonyl, an amide carbonyl, two  $\alpha,\beta$ -unsaturated  $\gamma$ -lactones, and a methoxy group. The above data indicated that **2** was also a dimeric securinine-type alkaloid. With the aid of 1D and 2D NMR experiments, the  $^1H$  and  $^{13}C$  NMR data of **2** were assigned and listed in Table S3.

The  $^1H$ - $^1H$  COSY correlations led to the establishment of four spin-coupling systems in **2**. In the HMBC spectrum, key correlations between  $H_2-5$  and  $C-3$ , between  $H_2-6$  and  $C-2$ , between  $H_2-7$  and  $C-2/C-6/C-9$ , between  $H_2-8$  and  $C-2/C-13$ , between  $H_2-12$  and  $C-9/C-14$ , between  $H_2-15$  and  $C-13$ , as well as between  $15-OCH_3$  and  $C-15$  suggested the existence of an unprecedented ring A opened 15-methoxy-14,15-dihydrosecurinine unit (**2a**). In addition, the HMBC correlations between  $H_2-2'$  and  $C-6'/C-8'/C-13'$ , between  $H_2-3'$  and  $C-9'$ , between  $H_2-7'$  and  $C-9'$ , between  $H_2-8'$  and  $C-13'/C-15'$ , between  $H_2-12'$  and  $C-9'$ , as well as between  $H_2-14'$  and  $C-7'/C-9'/C-12'$  established a phyllanthidine motif with a tetrahydro-1,2-oxazine ring (**2b**).<sup>9</sup> Furthermore, the HMBC correlations between  $H_2-7'/H_2-14'$  and  $C-3$  implied that two substructures **2a** and **2b** were also connected through the  $C-3-C-15'$  bond. Hence, the gross structure of **2** was established and shown in Figure 3.

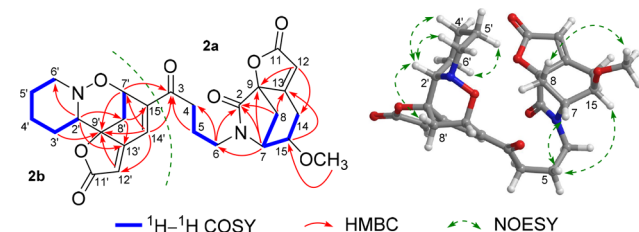


Figure 3. Key 2D NMR correlations of **2**.

The relative configuration of **2** could be determined by NOESY experiment as well as comparison of the NMR spectral data of **2** with those of the known compound. The NOE correlation between  $H_2-2'$  and  $H_2-8'a$  in the NOESY spectrum of **2**, as well as the significant similarities between the NMR data assigned to unit **2b** and those of phyllanthidine suggested that **2b** possessed consistent relative stereochemistry with phyllanthidine.<sup>9</sup> Besides, as depicted in the optimized molecular model of **2** (Figure 3), the NOE interactions between  $H_2-5$  and  $H_2-7/H_2-15$  as well as between  $15-OCH_3$  and  $H_2-8b$  indicated that  $15-OCH_3$  and the  $C-7-C-8-C-9$  carbon bridge were of the same orientation. To determine the absolute configuration of **2**, the theoretical ECD spectra of four possible stereoisomers of **2** were predicted by TDDFT calculation. Among the overall of predicted ECD spectra of four possible isomers of **2**, the calculated ECD curve of isomer 7*R*,9*R*,15*R*,2'*S*,7'*S*,9'*S*-**2** revealed a good agreement with the measured one (Figure S3A). Hence, the absolute configuration of **2** was assigned as 7*R*,9*R*,15*R*,2'*S*,7'*S*,9'*S*.

The molecular formula of flueggeacosine C (**3**) was determined to be  $C_{26}H_{28}N_2O_6$  on the basis of a quasi-molecular ion at  $m/z$  465.2020  $[M + H]^+$  (calcd for  $C_{26}H_{29}N_2O_6$ : 465.2026) in its HR-ESI-MS. The UV absorption maxima at 208 and 242 nm as well as IR bands at 3445, 1748, 1627, and 1436  $cm^{-1}$  implied the presence of a

hydroxyl group, a benzene ring, and an  $\alpha,\beta$ -unsaturated  $\gamma$ -lactone ring. The NMR spectra revealed that **3** possessed twenty-six carbons including a ketone carbonyl, two amide carbonyls, an  $\alpha,\beta$ -unsaturated  $\gamma$ -lactone ring, and a trisubstituted benzene ring.

The  $^1\text{H}$ - $^1\text{H}$  COSY spectrum of **3** revealed the existence of four spin-coupling systems as drawn in blue bold lines shown in Figure 4. In the HMBC spectrum, key correlations between

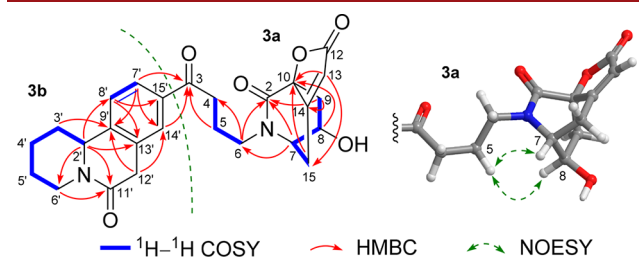


Figure 4. Key 2D NMR correlations of **3**.

$\text{H}_2$ -5 and C-3, between H-7 and C-2/C-6/C-14, between  $\text{H}_2$ -9 and C-2/C-14, between H-13 and C-10/C-15, and between  $\text{H}_2$ -15 and C-10 established a ring A opened neosecurinine motif (**3a**). Additionally, the HMBC correlations between H-2' and C-6'/C-8'/C-11'/C-13', between  $\text{H}_2$ -3' and C-9', between  $\text{H}_2$ -6' and C-11', between H-7' and C-9'/C-14', between H-8' and C-13'/C-15', as well as between  $\text{H}_2$ -12' and C-9'/C-14' revealed the existence of a benzoquinolizidine unit (**3b**). Moreover, the HMBC correlations between H-7'/H-14' and C-3 indicated that two substructures **3a** and **3b** were connected through C-3–C-15' bond.

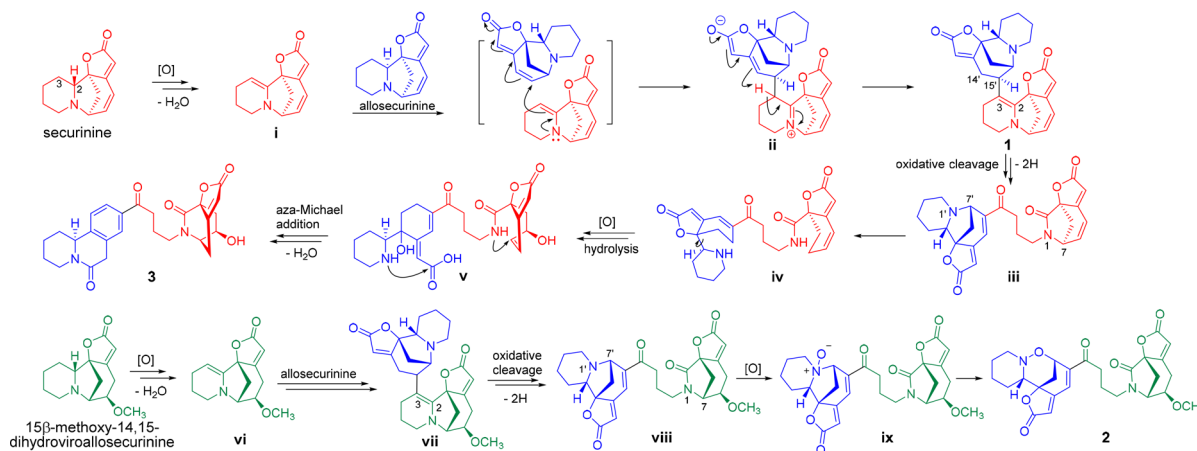
In the NOESY spectrum of **3**, the cross-peaks between  $\text{H}_2$ -5 and H-7/H-8 were observed, suggesting that those protons were of the same orientation. This assignment was supported by the predominant conformer obtained at the B3LYP/6-311++G(2d,p) level (Figure 4). Furthermore, the modified Mosher's method was applied to determine the absolute configuration of **3a**. Comparison of the  $^1\text{H}$  NMR chemical shift differences [ $\Delta\delta^{\text{SR}}$  ( $\delta\text{S} - \delta\text{R}$ )] between (*S*)- and (*R*)-MTPA esters of **3** led to the assignment of absolute configurations for 7*R*,8*R*,10*S* in **3** (Figure S4).<sup>10</sup> To further determine the stereochemistry of C-2', the theoretical optical rotation (OR) values of two possible absolute configurations of **3**, 7*R*,8*R*,10*S*,2'*S* (**3A**) and 7*R*,8*R*,10*S*,2'*R* (**3B**), were

calculated at B3LYP/6-311++G(2d,p), B3LYP/cc-pVDZ, and PBE0/def2-TZVP levels, respectively.<sup>6,11</sup> Using the corresponding lower energy conformations, the calculated OR magnitudes of **3A** ( $-72.6^\circ$ ,  $-78.3^\circ$ , and  $-71.5^\circ$ , respectively) were much closer to the recorded one ( $-74.1^\circ$ ) than those of **3B** ( $-48.4^\circ$ ,  $-17.2^\circ$ , and  $-25.8^\circ$ , respectively). Therefore, the absolute configuration of **3** was established as 7*R*,8*R*,10*S*,2'*S*. This assignment was subsequently confirmed by comparison of the calculated ECD spectrum with the experimental one of **3** (Figure S3B).

Compounds **1–3** represent three new classes of dimeric securinine-type alkaloid analogues. Based on the coexisting alkaloid monomers securinine (**4**), allosecurinine (**5**), and 15 $\beta$ -methoxy-14,15-dihydroviroallosecurinine (**6**, see the Supporting Information) in the same plant material, the hypothetical biogenetic pathways for **1–3** are proposed as shown in Scheme 1. Starting from the oxidation and dehydration of ring A of securinine, the key intermediate **i** could be yielded.<sup>3e,12</sup> Subsequently, allosecurinine could incorporate with enamine **i** through an electrophilic addition to produce **1**.<sup>5</sup> Oxidative cleavage of the C-2–C-3 double bond and dehydrogenation of C-14'–C-15' bond of **1** could lead to the generation of the ring A opened intermediate **iii**.<sup>13</sup> After the cleavage of the N-1–C-7 and N-1'–C-7' bonds,<sup>14</sup> intermediate **iv** could be formed. Further allylic oxidation of **iv** and subsequent hydrolysis could generate intermediate **v**, which could produce **3** through aza-Michael addition and lactam formation reactions. The formation of **2** might employ 15 $\beta$ -methoxy-14,15-dihydroviroallosecurinine and allosecurinine as the biosynthetic precursors. Through the similar procedures to **3**, intermediate **vii** could be obtained from the coupling of the two aforementioned putative precursors. Then, the oxidative cleavage of the C-2–C-3 double bond of **vii** and subsequent dehydrogenation could yield the ring A opened intermediate **viii**. Finally, intermediate **viii** could undergo an oxidation to form *N*-oxide **ix**, which could afford **2** through a rearrangement reaction.<sup>15</sup>

Neurite outgrowth is a crucial process during neuronal development and regeneration. Failure of this step normally leads to synapse dysfunction which contributes to a major pathogenesis cause of a wide variety of neurological diseases.<sup>16</sup> To explore the potential bioactivities of compounds **1–3** on neuronal differentiation, we took advantage of a mouse neuroblastoma cell model (Neuro-2a cells).<sup>17,18</sup> As a result,

### Scheme 1. Hypothetical Biogenetic Pathways for **1–3**





compounds 1–3 exhibited activities to promote the cells to differentiate into a neuron-like morphology, such as elongation of cell bodies and extension of neurites (Figure 5A). Relative

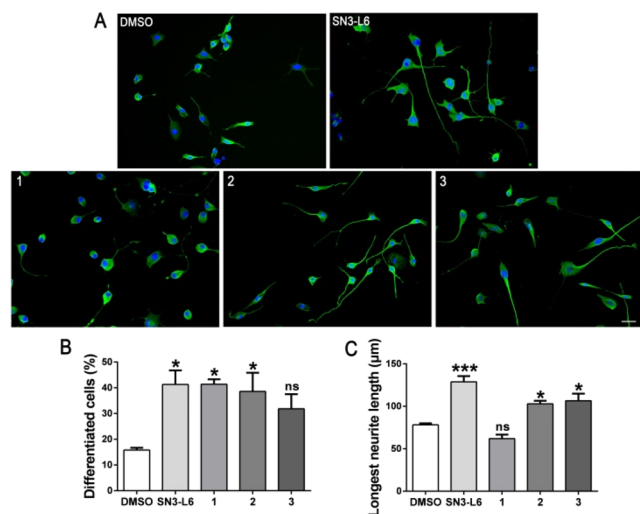


**Figure 5.** Compounds 1–3 promoted differentiation of Neuro-2a cells. (A) Neuro-2a cells were treated with 1–3 (25  $\mu$ M) or SN3-L6 (25  $\mu$ M) for 2 days. DMSO was a solvent control. Cells were immunostained using  $\beta$ -tubulin III antibody for visualization of neurites. Scale bar, 50  $\mu$ m. (B) Cell differentiation rate (% of cells that bear neurites). (C) Average length of the longest neurites. \* $p < 0.05$ , \*\* $p < 0.01$ , \*\*\* $p < 0.001$ , one way analysis of variance (ANOVA) with a Dunnett's multiple comparisons test, at least 400 cells/group were analyzed in each experiment,  $n = 4$ . Error bars indicate  $\pm$  SEM.

to 1 and 3, statistical analysis showed that 2 has better neuronal differentiation activity, as 2 not only induced more cells to differentiate, but also promoted the extension of neurites (Figures 5B and 5C). The activity of 2 was comparable to SN3-L6, a synthetic compound regarding as a potent neuritogenesis,<sup>18</sup> which suggested that 2 might provide a potentially new structure for future drug design of diseases involving disrupted neuronal differentiation.

## ■ ASSOCIATED CONTENT

### Supporting Information

The Supporting Information is available free of charge on the ACS Publications website at DOI: 10.1021/acs.orglett.8b03432.

Detailed descriptions of the experimental procedure; UV, IR, MS, and NMR spectra for compounds 1–6; DFT calculations for 2 and 3 (PDF)

## Accession Codes

CCDC 1819362 contains the supplementary crystallographic data for this paper. These data can be obtained free of charge via [www.ccdc.cam.ac.uk/data\\_request/cif](http://www.ccdc.cam.ac.uk/data_request/cif), or by emailing [data\\_request@ccdc.cam.ac.uk](mailto:data_request@ccdc.cam.ac.uk), or by contacting The Cambridge Crystallographic Data Centre, 12 Union Road, Cambridge CB2 1EZ, UK; fax: +44 1223 336033.

## ■ AUTHOR INFORMATION

### Corresponding Authors

\*E-mail: [wangying\\_cpu@163.com](mailto:wangying_cpu@163.com) (Y.W.)

\*E-mail: [chywc@aliyun.com](mailto:chywc@aliyun.com) (W.-C.Y.)

## ORCID

Zhen-Long Wu: 0000-0001-8985-7980

Xiao-Jun Huang: 0000-0002-3636-4813

Wen-Cai Ye: 0000-0002-2810-1001

Ying Wang: 0000-0003-4524-1812

## Author Contributions

<sup>§</sup>Z.-L.W. and X.-J. H. contributed equally to this work.

## Notes

The authors declare no competing financial interest.

## ■ ACKNOWLEDGMENTS

This work was financially supported by the National Natural Science Foundation of China (Nos. 81630095, 81803379, 81622045, and 81473117) and the Science and Technology Planning Project of Guangdong Province (2016B030301004).

## ■ REFERENCES

- (1) For reviews on the *Securinega* alkaloids, see: (a) Weinreb, S. M. *Nat. Prod. Rep.* **2009**, *26*, 758–775. (b) Chirkin, E.; Atkalian, W.; Porée, F. H. *Alkaloids. Chemistry and Biology* **2015**, *74*, 1–120. (c) Wehlauch, R.; Gademann, K. *Asian J. Org. Chem.* **2017**, *6*, 1146–1159.
- (2) (a) Neganova, M. E.; Sercova, T. P.; Shevtsova, E. F.; Klochkov, S. G.; Bachurin, S. J. *Neurochem.* **2009**, *110*, 10–18. (b) Gupta, K.; Chakrabarti, A.; Rana, S.; Ramdeo, R.; Roth, B. L.; Agarwal, M. L.; Tse, W.; Agarwal, M. K.; Wald, D. N. *PLoS One* **2011**, *6*, No. e21203. (c) Vu, H.; Roullier, C.; Campitelli, M.; Trenholme, K. R.; Gardiner, D. L.; Andrews, K. T.; Skinner-Adams, T.; Crowther, G. J.; Van Voorhis, W. C.; Quinn, R. J. *ACS Chem. Biol.* **2013**, *8*, 2654–2659.
- (3) (a) Ohsaki, A.; Kobayashi, Y.; Yoneda, K.; Kishida, A.; Ishiyama, H. *J. Nat. Prod.* **2007**, *70*, 2003–2005. (b) Zhao, B. X.; Wang, Y.; Zhang, D. M.; Huang, X. J.; Bai, L. L.; Yan, Y.; Chen, J. M.; Lu, T. B.; Wang, Y. T.; Zhang, Q. W.; Ye, W. C. *Org. Lett.* **2012**, *14*, 3096–3099. (c) Wu, Z. L.; Zhao, B. X.; Huang, X. J.; Tang, G. Y.; Shi, L.; Jiang, R. W.; Liu, X.; Wang, Y.; Ye, W. C. *Angew. Chem., Int. Ed.* **2014**, *53*, 5796–5799. (d) Zhang, H.; Zhu, K. K.; Han, Y. S.; Luo, C.; Wainberg, M. A.; Yue, J. M. *Org. Lett.* **2015**, *17*, 6274–6277. (e) Luo, X. K.; Cai, J.; Yin, Z. Y.; Luo, P.; Li, C. J.; Ma, H.; Seeram, N. P.; Gu, Q.; Xu, J. *Org. Lett.* **2018**, *20*, 991–994.
- (4) For selected examples, see: (a) Gan, L. S.; Fan, C. Q.; Yang, S. P.; Wu, Y.; Lin, L. P.; Ding, J.; Yue, J. M. *Org. Lett.* **2006**, *8*, 2285–2288. (b) Zhao, B. X.; Wang, Y.; Zhang, D. M.; Jiang, R. W.; Wang, G. C.; Shi, J. M.; Huang, X. J.; Chen, W. M.; Che, C. T.; Ye, W. C. *Org. Lett.* **2011**, *13*, 3888–3891. (c) Zhang, H.; Zhang, C. R.; Zhu, K. K.; Gao, A. H.; Luo, C.; Li, J.; Yue, J. M. *Org. Lett.* **2013**, *15*, 120–123. (d) Zhang, H.; Han, Y. S.; Wainberg, M. A.; Yue, J. M. *Tetrahedron* **2015**, *71*, 3671–3679.
- (5) Jeon, S. B.; Han, S. K. *J. Am. Chem. Soc.* **2017**, *139*, 6302–6305.
- (6) Zhao, B. X.; Wang, Y.; Li, C.; Wang, G. C.; Huang, X. J.; Fan, C. L.; Li, Q. M.; Zhu, H. J.; Chen, W. M.; Ye, W. C. *Tetrahedron Lett.* **2013**, *54*, 4708–4711.
- (7) Kumarasamy, E.; Raghunathan, R.; Sibi, M. P.; Sivaguru, J. *Chem. Rev.* **2015**, *115*, 11239–11300.
- (8) Johnson, E. R.; Keinan, S.; Mori-Sanchez, P.; Contreras-Garcia, J.; Cohen, A. J.; Yang, W. *J. Am. Chem. Soc.* **2010**, *132*, 6498–6506.
- (9) Chirkin, E.; Atkalian, W.; Do, Q.; Gaslonde, T.; Dufat, T.; Michel, S.; Lemoine, P.; Genta-Jouve, G.; Poree, F.-H. *Nat. Prod. Res.* **2015**, *29*, 1235–1242.
- (10) Hoyer, T. R.; Jeffrey, C. S.; Shao, F. *Nat. Protoc.* **2007**, *2*, 2451–2458.
- (11) (a) Dong, L. B.; Gao, X.; Liu, F.; He, J.; Wu, X. D.; Li, Y.; Zhao, Q. S. *Org. Lett.* **2013**, *15*, 3570–3573. (b) Hashmi, M. A.; Andressend, S. K.; Keyzers, R. A.; Lein, M. *Phys. Chem. Chem. Phys.* **2016**, *18*, 24506–24510.

(12) Arata, Y.; Yoshifuji, S.; Yasuda, Y. *Chem. Pharm. Bull.* **1969**, *17*, 1363–1368.

(13) (a) Lara, M.; Mutti, F. G.; Glueck, S. M.; Kroutil, W. J. *Am. Chem. Soc.* **2009**, *131*, 5368–5369. (b) Bugg, T. D. H. *Tetrahedron* **2003**, *59*, 7075–7101.

(14) Arbain, D.; Girkbeck, A. A.; Byrne, L. T.; Sargent, M. V.; Skelton, B. W.; White, A. H. *J. Chem. Soc., Perkin Trans. 1* **1991**, 1863–1869.

(15) Li, J. Y.; Zhao, B. X.; Zhang, W.; Li, C.; Huang, X. J.; Wang, Y.; Sun, P. H.; Ye, W. C.; Chen, W. M. *Tetrahedron* **2012**, *68*, 3972–3979.

(16) Krstic, D.; Knuesel, I. *Nat. Rev. Neurol.* **2013**, *9*, 25–34.

(17) Xiao, Y. G.; Peng, Y. H.; Wan, J.; Tang, G. Y.; Chen, Y. W.; Tang, J.; Ye, W. C.; Ip, N. Y.; Shi, L. *J. Biol. Chem.* **2013**, *288*, 20034–20045.

(18) (a) Tang, G. Y.; Liu, X.; Ma, N.; Huang, X. J.; Wu, Z. L.; Zhang, W.; Wang, Y.; Zhao, B. X.; Wang, Z. Y.; Ip, F. C.F.; Ip, N. Y.; Ye, W. C.; Shi, L.; Chen, W. M. *ACS Chem. Neurosci.* **2016**, *7*, 1442–1451. (b) Liao, Y. M.; Zhuang, X. J.; Huang, X. J.; Peng, Y. H.; Ma, X. Y.; Huang, Z. X.; Liu, F.; Xu, J.; Wang, Y.; Chen, W. M.; Ye, W. C.; Shi, L. *Front. Pharmacol.* **2018**, *9*, 290.